

Microhardness, toughness, and modulus of Mohs scale minerals

MARGARET E. BROZ,^{1,*} ROBERT F. COOK,¹ AND DONNA L. WHITNEY²

¹Department of Chemical Engineering and Materials Science, University of Minnesota, Minneapolis, Minnesota 55455, U.S.A.

²Department of Geology and Geophysics, University of Minnesota, Minneapolis, Minnesota 55455, U.S.A.

ABSTRACT

We report new results of microhardness and depth-sensing indentation (DSI) experiments for the first nine minerals in the Mohs scale: talc, gypsum, calcite, fluorite, apatite, orthoclase, quartz, topaz, and corundum. The Mohs scale is based on a relative measure of scratch resistance, but because scratching involves both loading and shearing, scratch resistance is not equivalent to hardness as measured by modern loading (indentation) methods; scratch resistance is also related to other material properties (fracture toughness, elastic modulus). To better understand the relationship of hardness to scratch resistance, we systematically determined hardness, fracture toughness, and elastic modulus for Mohs minerals. We measured hardness and toughness using microindentation, and modulus and hardness with DSI (“nanoindentation”) experiments. None of the measured properties increases consistently or linearly with Mohs number for the entire scale.

Keywords: Mechanical properties, hardness, fracture toughness, elastic modulus, Mohs minerals, new technique, nanoindentation

INTRODUCTION

The Mohs scale has been a part of geoscience research and teaching for nearly two centuries. Originally developed as a guide for mineral identification, it qualitatively ranks ten standard minerals according to their increasing resistance to scratching with a file or other standard mineral. The degree of scratch resistance is judged by the width and depth of the residual scratch, but there is no systematic method of testing (Mohs 1825). This measurement of scratch resistance is frequently referred to as hardness, and varies with crystal orientation in minerals—including isometric minerals—because atomic structure and bonding characteristics vary in different directions. Scratch resistance is related to hardness, which is resistance to plastic (permanent) deformation, but the Mohs scale is not technically a hardness scale because resistance to scratching of brittle materials is a complex function of a combination of factors, including hardness, fracture toughness, and elastic modulus. Because scratch resistance and the modern definition of hardness are not equivalent, their relationship needs to be explored.

Hardness is the resistance of a material to permanent (plastic) deformation, or, the mean supported contact stress under a static local load (Hertz 1896; Williams 1942; Tabor 1970; Oliver and Pharr 1992). Hardness therefore lends itself to quantitative measurement using static indentation experiments, but not necessarily to development of a quantitative hardness scale because hardness values are a function of the experimental parameters (e.g., indenter shape, dwell time, etc.). Conventional indentation experiments involve applying and removing a specified load onto a flat, polished surface of a specimen via an indenter probe. Measurement of the residual plastic deformation zone yields hardness, while measurement of the length of cracks often generated at the contact relates to the fracture toughness (resistance

to fracture) of the material.

Many researchers have studied the hardness of the Mohs minerals using a variety of techniques, and it is well known that the minerals in the Mohs scale do not increase linearly in hardness (e.g., Hodge and McKay 1934; Knoop et al. 1939). However, scratch resistance is not dependent on hardness alone; it is a complicated function of hardness, fracture toughness, elastic modulus (resistance to elastic deformation), and loading method. To develop a better understanding of the mechanics of scratch resistance, we performed microindentation and depth-sensing indentation (DSI) experiments to quantify various physical properties of nine of the Mohs minerals, excluding diamond: talc, gypsum, calcite, fluorite, apatite, orthoclase (feldspar), quartz, topaz, and corundum. Our aims were to determine what parameters influence the scratch resistance of minerals, and to use our quantitative data for mineral properties (hardness, toughness, modulus) to evaluate why the Mohs minerals have a theoretical linearity according to the qualitative scale.

OVERVIEW OF HARDNESS AND RELATED PROPERTIES

Geoscientists use resistance to scratching as a proxy for hardness because a qualitative scratching scale is a useful tool for mineral identification and is amenable to wide use. Quantitative values for hardness do not increase linearly with Mohs hardness number, implying that scratch resistance depends on hardness—and modulus and toughness—in a complicated manner. Other considerations, such as the effect of the coefficient of friction, porosity, and strain hardening characteristics may also play a role.

Because of the long history of qualitative hardness testing of minerals, a century of quantitative hardness testing, and recent advances in DSI (“nanoindentation”) techniques, it is useful to survey the evolution of these techniques and describe current methods, including those used in the present study.

* E-mail: broz@cems.umn.edu

A brief history of hardness testing

The property of mineral hardness has long been used to identify minerals. Theophrastus, a student of Aristotle, published the earliest known reference to a property called mineral hardness in his treatise "On stones" (ca. 305–315 BCE) (Caley and Richards 1956). Almost 400 years later, Pliny the Elder noted, in the last volume of his 37-volume "Natural History", that minerals exhibit a wide range of hardness (Pliny 77; Eichholz 1971).

R.A.F. de Réaumur (1722, see Sisco 1956), the French scientist who experimented with the structure and properties of metals (and insects), was the first to describe systematic scratch testing. In his treatise on iron and steel (*L'Arte de convertir le fer forge en acier*), he described the results of scratching a metal bar that was graduated in hardness along its length, having been mildly quenched at one end. In addition, he devised a scheme using a variety of stones to differentiate the hardness of steels that were harder than normal files.

In 1774, A.G. Werner published a book, *Von den äusserlichen Kennzeichen der Fossilien (On the External Characters of Minerals)*, translated into English in 1962, in which he classified minerals based on their external characteristics, including resistance to scratching by a file, knife, or steel tool. He separated minerals into four categories: hard, semihard, soft, and very soft, and provided a long list of minerals that fit into each category. The "hard" category was further divided into how a mineral responded to a file, and ranged from garnet (which was considered softer than quartz) and feldspar at the lower end to corundum and diamond at the high end.

In the early 1800s, R.-J. Haüy, who is well known for his work on crystal forms, proposed a more complicated classification of mineral hardness. In *Traité de Minéralogie* (1822), Haüy described four divisions of hardness, using quartz, glass, and calcite as standards, and he described various testing methods involving scratching an unknown mineral with the corner or edge of a file, with the point or blade of a steel tool, or with the corner of another mineral (Haüy 1822; Hooymaas 1970).

Friedrich Mohs studied with Werner in Freiberg, Germany, and published his own Treatise (1822, translated to English in 1825), in which he meticulously described and classified many physical properties of minerals, including hardness. Mohs defined hardness as "the resistance of solid minerals to the displacement of their particles" (Mohs 1825). He developed his scale because no accurate method for measuring hardness existed at that time, and he stressed the point that in the absence of an accurate test, a relative one would be invaluable.

Mohs took great care in selecting the minerals in his scale: talc, gypsum, calcite, fluorite, apatite, orthoclase, quartz, topaz, corundum, and diamond. In his selection, he considered the availability of the minerals (he chose common minerals that were fairly easy to acquire), and he tried to make the minerals in the scale as uniformly spaced as possible in terms of their scratch resistance. Mohs' selection of minerals for his scale was excellent: the "hardness" interval between any two members of the scale is enough so that they can be easily distinguished from each other, but not so close that using the scale is difficult. Further testament to the success of his efforts is the fact that half units can be assigned to some minerals, although Mohs himself was more optimistic and believed that the intervals between any two

consecutive minerals in the scale could be divided into tenths.

In 1900, J.A. Brinell developed a quantitative method for determining the hardness of metals by forcing a hardened steel ball into a flat surface of a specimen at a specific load. He calculated hardness (known today as the Brinell Hardness, HB) from the diameter of the impression, the diameter of the ball, and load (Williams 1942). In 1922, S.P. Rockwell expanded on Brinell's indentation method and experimented with various loads and indenters of different diameters (Rockwell 1922). Different scales arose from the different parameters used.

These techniques work well for metals, but more brittle materials such as non-metallic minerals and ceramics shatter under the loads used by Brinell and Rockwell indenters (>500 N). Hodge and McKay (1934) published a groundbreaking paper discussing the use of reproducible scratching as a test for mineral hardness. Using a cube-corner diamond and an instrument called a microcharacter, they made scratches in minerals at light loads. They reported data from a series of parallel and perpendicular scratches for the first nine Mohs minerals. Hardness was calculated from the reciprocal of the width of the scratch, and results yielded an approximate logarithmic fit of Mohs number plotted vs. hardness. Tabor (1951) also investigated scratch hardness of the Mohs minerals, and reported a logarithmic trend of Mohs number with scratch hardness.

Experimental techniques for the indentation of brittle materials were further developed in the 20th century. For example, Knoop et al. (1939) described a pyramidal diamond indenter probe that could be operated at light loads (<10 N). Similar techniques are used today; two of the most common probe geometries are the Vickers four-sided diamond pyramid and the Berkovich three-sided diamond pyramid. Various studies have tested the Mohs minerals with these probe geometries and noted that the scale is not linear (Knoop et al. 1939; Winchell 1945; Taylor 1949; Khrushchov 1949, 1950; Tabor 1954; West 1986).

In the last two decades, depth-sensing indentation has been developed and widely applied to the characterization of solid materials and thin films. This technique, which is described in the next section, has an important advantage over more traditional indentation experiments because the load and depth into the sample is continuously measured, allowing for the quantification of elastic recovery.

Determination of material properties using Mohs, microindentation, and depth-sensing indentation methods

In the Mohs method, a sharp corner of a standard mineral or knife is pushed into a smooth, flat face of the mineral to be tested (Mohs 1825) (Fig. 1a). Load is applied onto the sample as well as transversely across its face. Elastic and plastic deformation and fracture occurs during loading. After scratching, if the sample has a lower Mohs number than the scratching tool, a scratch will be visible on the sample surface, the depth and width of which can be used in refining the qualitative assessment of the Mohs hardness.

Microindentation is a static indentation method involving applying and removing a specified load onto a sample by an indenter (probe), typically made of diamond. During loading, the sample plastically and elastically deforms, and on unloading, it recovers elastically. A visible light microscope can usually measure the

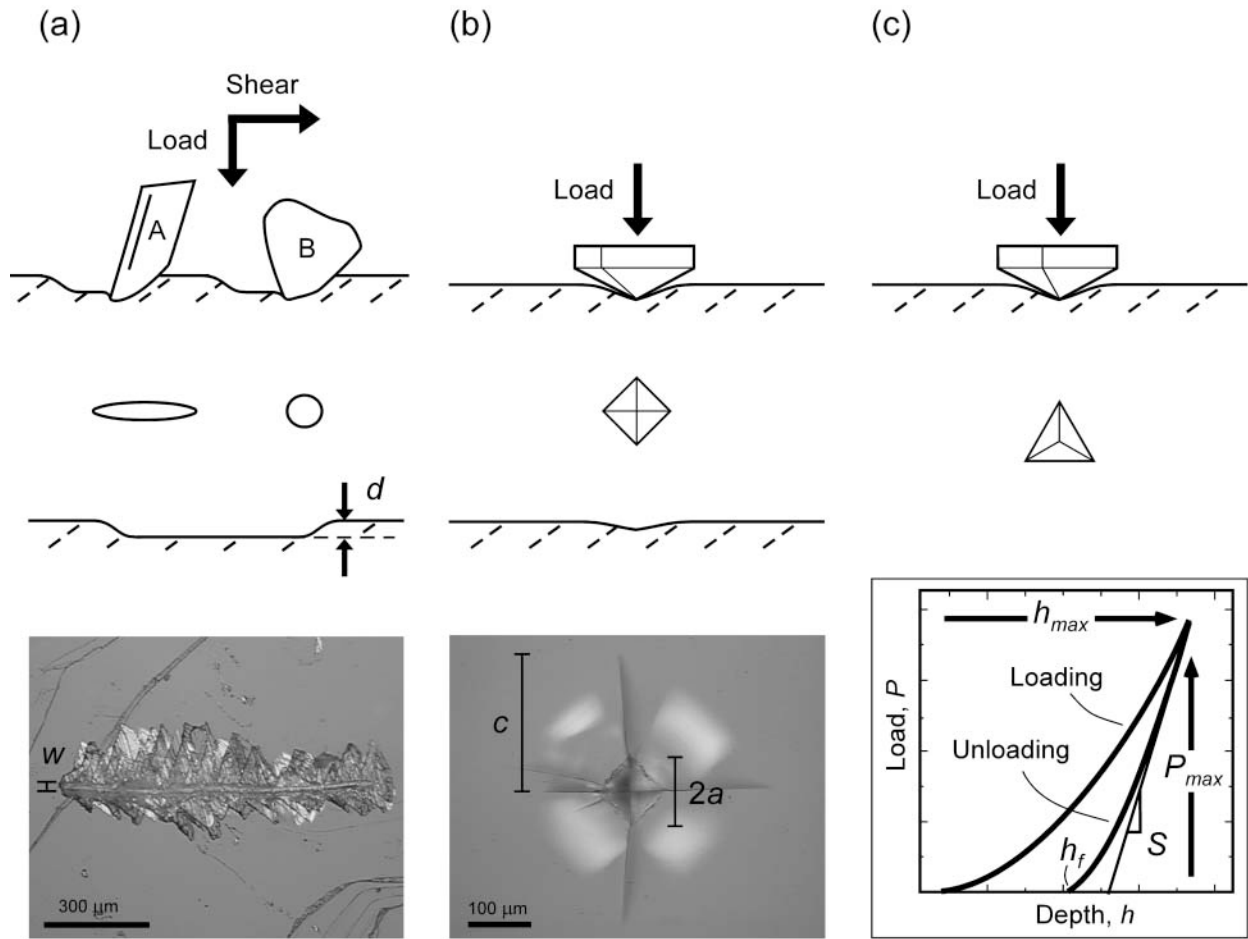


FIGURE 1. Schematic representations of methods for determining mineral hardness. (a) The Mohs scratch test involves scratching a knife (A) or another mineral (B) against the unknown mineral, as shown in cross section (top panel), and top view using a knife or roughly circular tool (second panel). The geometry of a typical scratch is shown in cross section (third panel) and in an optical image of a scratch in calcite (bottom panel); w , the width of the scratch and d , the depth of the scratch, together are qualitative measures of scratch resistance. (b) Microindentation involves forcing a diamond tip into a mineral (top panel) at known load, here using a Vickers indenter (top view in second panel). The geometry of a typical indentation is shown in cross section (third panel) and in an optical image of an indentation in soda-lime glass, with c = crack length and $2a$ = dimension of the contact impression. (c) Depth-sensing indentation also involves forcing a diamond tip into a mineral (top panel), here using a Berkovich indenter (top view in second panel). The load and penetration depth are constantly monitored, resulting in a curve for the loading-unloading cycle (bottom panel).

dimensions of the residual indentation impression and any cracks that formed, which are then used to calculate hardness (Hertz 1896; Tabor 1951, 1970; Lawn et al. 1980) and toughness (Lawn et al. 1980; Anstis et al. 1981; Cook et al. 1985) (Fig. 1b). In the case of a Vickers indenter, hardness, H , is determined by

$$H = \frac{P}{2(a^2)} \quad (1)$$

where P is the applied load and a is half of the residual contact diagonal, recognizing that hardness is the load divided by the mean supported contact area, which is calculated here using the contact diagonal.

Microindentation of brittle materials also often results in cracking (Fig. 1b). Fracture toughness, K_{Ic} can be related empirically to the length of radial cracks (described below) produced by a Vickers indenter:

$$K_{Ic} = 0.022 \left(\frac{E}{H} \right)^{1/2} \frac{P}{c^{3/2}} \quad (2)$$

where E is the elastic modulus and c is the radial crack length (Lawn et al. 1980; Anstis et al. 1981; Cook et al. 1985).

DSI involves applying and removing a load on a sample via an indenter, but differs from microindentation because DSI measurements are taken *during* the indentation event: the DSI apparatus continuously measures the penetration depth (displacement) of the indenter into the surface and the force (load) applied to the sample (Fig. 1c), whereas microindentation measurements are taken after the indentation event. The characteristic shape of the load-displacement curves depends on indenter geometry, ambient temperature, and the mechanical properties of the material. DSI data can be used to calculate the elastic modulus because no plastic deformation is assumed on unloading, allowing for

the elastic and plastic indentation responses of the material to be considered separately (Oliver and Pharr 1992).

Analysis of the continuous load-displacement data from DSI yields modulus, E' , and hardness, H , values according to the equations below.

Hertz (1896) introduced the reduced modulus, E_r , to account for the effects of a non-rigid indenter on the measured load-displacement behavior:

$$\frac{1}{E_r} = \frac{(1-\nu^2)}{E} + \frac{(1-\nu_i^2)}{E_i} \quad (3)$$

where E and ν are the elastic modulus and Poisson's ratio for the sample, and E_i and ν_i are the same parameters for the indenter material (Oliver and Pharr 1992).

The experimentally measured unloading contact stiffness, S , is related to P and displacement, h :

$$S = \frac{dP}{dh} = \frac{E_r \sqrt{A} \sqrt{\pi}}{2} \quad (4)$$

where A is the projected area of contact with the indenter.

Accordingly, the reduced modulus can be calculated by

$$E_r = \frac{\sqrt{\pi}}{2} \frac{S}{\sqrt{A}} \quad (5)$$

Following the method of Oliver and Pharr (1992), S can be calculated using an upper portion of the unloading data, which is described by $P = \alpha(h - h_f)^m$, where h_f is the final depth and α and m are two empirically derived constants. As $S = dP/dh$, analytical differentiation is used to calculate the experimentally measured stiffness:

$$S = \alpha m (h - h_f)^{m-1}. \quad (6)$$

Knowing S , one can calculate h_c , the contact depth:

$$h_c = h_{\max} - \frac{0.75 P_{\max}}{S} \quad (7)$$

where h_{\max} is the maximum displacement into the sample surface at the maximum applied load, P_{\max} , and 0.75 is a geometric constant.

The parameter A , the projected area of contact, depends on geometric constants and h_c :

$$A = C_0 h_c^2 + C_1 h_c + C_2 h_c^{1/2}. \quad (8)$$

C_0 , C_1 , and C_2 are area coefficients for the specific indenter geometry employed. The first term describes the shape of the indenter ($C_0 = 24.5$ nm for a Berkovich indenter), and the others account for geometrical imperfections, such as tip blunting. C_1 and C_2 are determined through a series of calibration experiments using standard materials.

Once the parameters described above are calculated, the reduced modulus is given by:

$$\frac{1}{E_r} = \left(\frac{1}{S^{-1} - C_f} \right) \left(\frac{\sqrt{\pi}}{2\sqrt{A}} \right) \quad (9)$$

where C_f is the frame compliance and other variables are as defined above.

In the case where the Poisson's ratio for the sample is unknown, the modulus is usually reported as the plane strain elastic modulus, E' :

$$\frac{1}{E'} = \frac{1}{E_r} - \frac{(1-\nu_i^2)}{E_i}. \quad (10)$$

Hardness can be calculated by

$$H = \frac{P_{\max}}{A} \quad (11)$$

where A is calculated using Equation 8.

MICROINDENTATION AND DSI OF THE MOHS MINERALS

The minerals in the Mohs scale vary greatly in their composition and structure. The scale includes silicates and non-silicates, and crystal symmetry ranging from isometric (fluorite, diamond) to monoclinic (talc, gypsum, orthoclase) (Table 1).

Materials and methods

Most of the minerals obtained in a commercial Mohs testing kit were not suitable for our study because of high levels of impurities, particularly for talc. Information about our specific samples is given in Table 2.

Samples were cut or broken along cleavage planes where possible, and sawed along the basal plane for apatite and quartz. For fluorite and topaz, we confirmed the orientation of the plane using electron back-scattered diffraction (EBSD).

With the desired plane facing out, samples were embedded in epoxy and highly polished. The microindentation experiments were performed with a Buehler Micromet 2103 MMT-7 microhardness tester, using a Vickers (four-sided pyramid) diamond indenter probe at ambient conditions in air. We made five microindentations on one sample of each mineral at three loads (typically 0.5, 1, and 2 N). Crack lengths and contact impression dimensions were measured for each indentation using the optics on the Micromet. Images of the indentation flaws were taken using an inverted visible light microscope running MetaMorph 4.1 software or with a

TABLE 1. Mohs minerals compositions and crystal structures

Mohs number	Mineral	Chemical formula	Crystal system	Cleavage
1	talc	$Mg_3Si_4O_{10}(OH)_2$	monoclinic	perfect {001}
2	gypsum	$CaSO_4 \cdot 2H_2O$	monoclinic	perfect {010}, good {100}
3	calcite	$CaCO_3$	trigonal	perfect {1010}
4	fluorite	CaF_2	isometric	perfect {111}
5	apatite	$Ca_5(PO_4)_3F$	hexagonal	poor {001}
6	orthoclase	$KAlSi_3O_8$	monoclinic	perfect {001}, good {010}
7	quartz	SiO_2	trigonal	none
8	topaz	$Al_2SiO_4(OH,F)_2$	orthorhombic	perfect {0001}
9	corundum	Al_2O_3	trigonal	none
10	diamond	C	isometric	perfect {111}

TABLE 2. The names, descriptions, and indentation planes of samples used for this study

Mineral	Description	Indentation plane
talc	White, massive Mg end-member with randomly oriented crystals. We were not able to separate an individual crystal, so indented the poly-crystalline mass.	
gypsum	Clear crystal with obvious cleavage planes.	{010}
calcite	Translucent cleavage rhomb.	{1010}
fluorite	Translucent purple crystals.	{111}
apatite	Fluorapatite variety (< 0.45 wt% Cl), yellow hexagonal prism from Durango, Mexico.	{0001}
orthoclase	Pink-orange, minor perthite texture, one obvious cleavage.	{101}
quartz	Clear prismatic with crystal faces.	{0001}
topaz	Clear prismatic with crystal faces.	{001}
corundum	Clear synthetic crystal.	{0001}

scanning electron microscope (JEOL JSM-6500 FEG-SEM).

The DSI experiments were performed on a NanoIndenter XP running TestWorks 4.0 software, using a Berkovich (3 sided pyramid) diamond at ambient conditions in air. Each sample was tested at least eight times. All experiments employed a constant loading and unloading rate of 1 mN/sec for 100 sec, yielding a peak load of 100 mN.

Results

Each Mohs mineral responds differently to indentation, as is evident by the clarity of contact impression edges, and the length, number, direction, and type (radial and lateral) of cracks produced by microindentation (Fig. 2). Radial cracks emanate from the corners of the contact impression (perpendicular to the sample surface), are generally straight and appear dark, as in Figure 2g, while lateral cracks emanate from below the contact impression (parallel to the sample surface), are roughly circular, and appear bright, as in Figure 2e. Using the methods and equations described, we calculated hardness and toughness from the microindentation experiments, and hardness and modulus from the DSI experiments (Table 3).

Microhardness values for the Mohs minerals show a stepwise increase in hardness across the scale (see Fig. 3a). Talc, gypsum, calcite, and fluorite all have hardness ~ 2 GPa, but there is a

larger jump between fluorite (Mohs number = 4; $H = 2.00$ GPa) and apatite (Mohs number = 5; $H = 5.43$ GPa). After a modest increase between apatite and orthoclase (Mohs number = 6; $H = 6.87$ GPa), there is another large jump in values between orthoclase and quartz (Mohs number = 7; $H = 12.2$ GPa). Hardness continues increasing by a similar degree between quartz and topaz (Mohs number = 8; $H = 17.6$ GPa), then increases

TABLE 3. Physical properties of the Mohs minerals

Mohs number	Mineral	Microhardness (GPa)	DSI hardness (GPa)	DSI modulus (GPa)	Toughness ($\text{MPa} \cdot \text{m}^{1/2}$)
1	talc	0.14 ± 0.03	0.30 ± 0.18	16.2 ± 6.6	–
2	gypsum	0.61 ± 0.15	1.03 ± 0.13	25.3 ± 1.9	–
3	calcite	1.49 ± 0.11	2.21 ± 0.16	78.1 ± 5.2	0.39 ± 0.12
4	fluorite	2.00 ± 0.10	2.37 ± 0.02	139.7 ± 3.8	0.89 ± 0.13
5	apatite	5.43 ± 0.33	6.73 ± 0.38	150.8 ± 6.4	0.76 ± 0.13
6	orthoclase	6.87 ± 0.66	9.11 ± 0.58	89.2 ± 7.1	0.88 ± 0.13
7	quartz	12.2 ± 0.6	14.54 ± 0.42	117.6 ± 2.7	1.60 ± 0.16
8	topaz	17.6 ± 1.0	21.38 ± 1.32	268.8 ± 5.6	1.04 ± 0.10
9	corundum	19.6 ± 0.5	29.29 ± 0.45	376.1 ± 9.8	2.38 ± 0.22
10	diamond	(115*)	–	(1050†)	(5*)

Note: Uncertainties listed are one standard deviation.

* Values from Novikov and Dub (1991).

† Value from Kong and Ashby (1992).

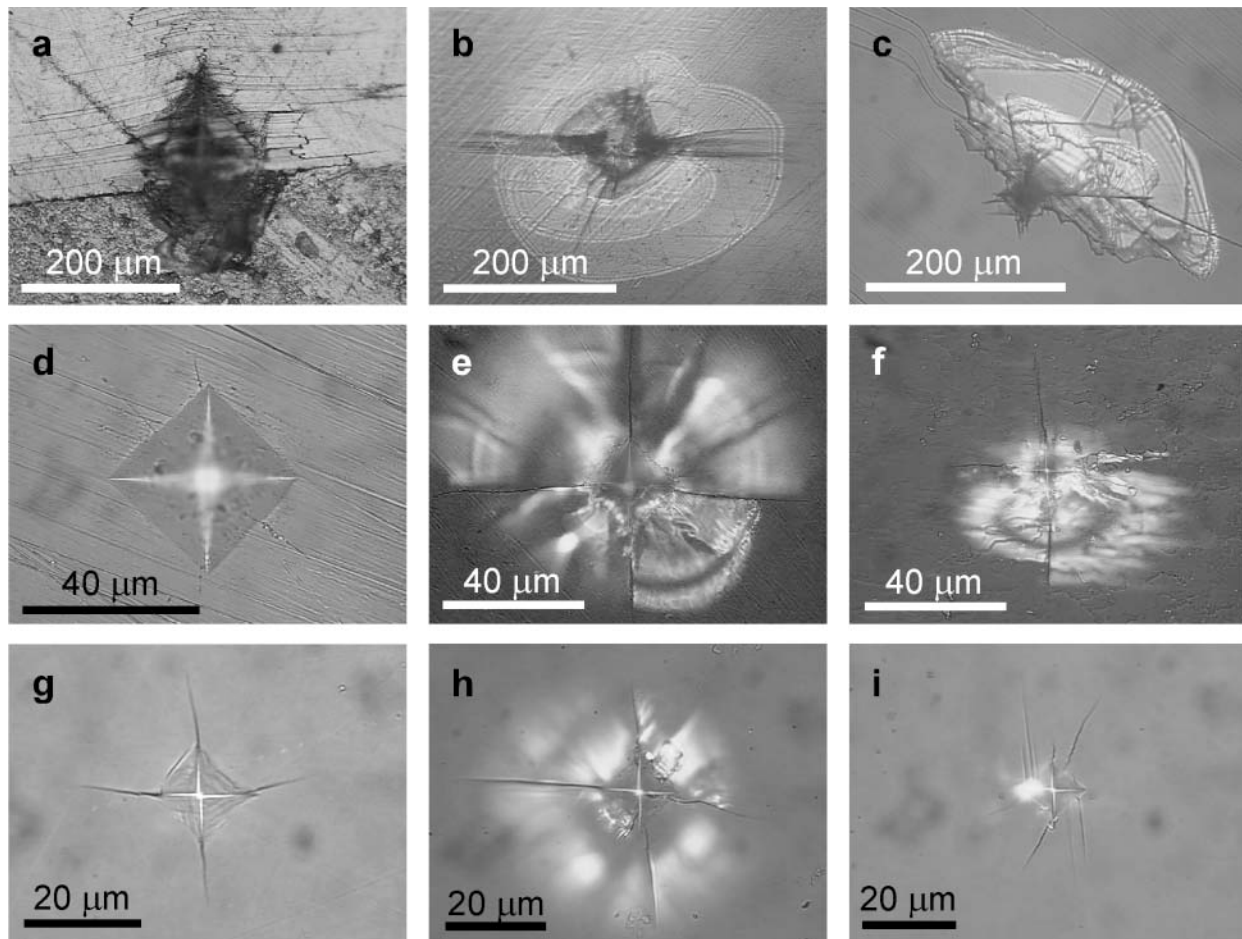


FIGURE 2. Contact impressions from microhardness experiments for the Mohs minerals, all at $P = 2$ N: (a) talc, (b) gypsum, (c) calcite, (d) fluorite, (e) apatite, (f) orthoclase, (g) quartz, (h) topaz, and (i) corundum.

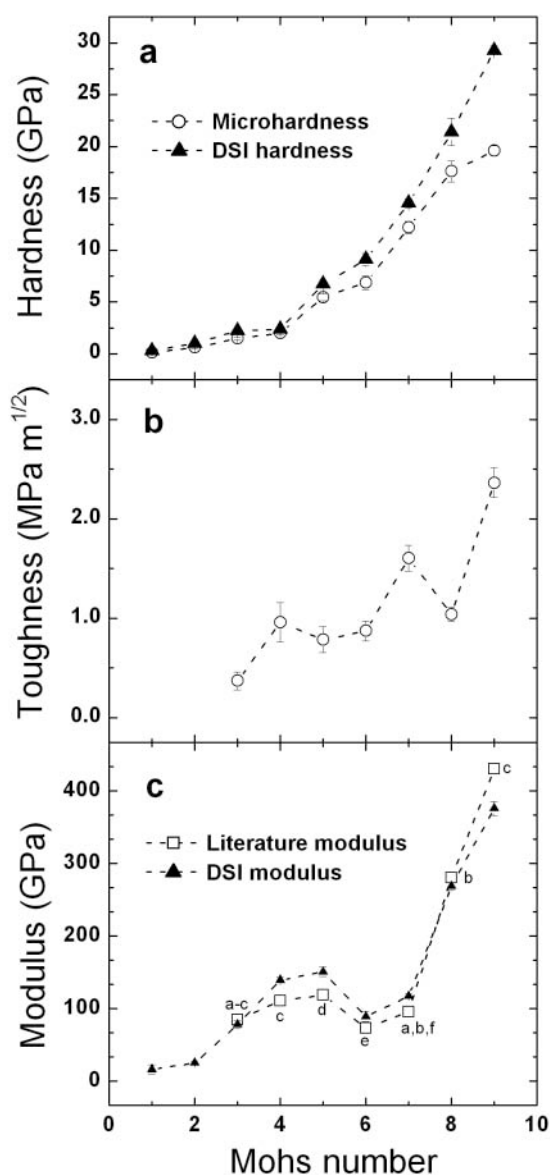


FIGURE 3. (a) Microhardness and DSI hardness vs. Mohs number, (b) Toughness vs. Mohs number, (c) Experimental and literature modulus vs. Mohs number. References for literature values listed next to each point: a = Alexandrov and Ryzhova (1961); b = Hearmon (1946); c = Hearmon (1956); d = Yoon and Newnham (1969); e = Alexandrov and Ryzhova (1962); f = Huntington (1958). Dashed lines are guides to the eye and do not imply trends.

modestly to corundum (Mohs number = 9; $H = 21.22$ GPa). A literature value for diamond (Mohs number = 10) lists $H = 115$ GPa, an almost sixfold increase from corundum.

As observed elsewhere, the DSI hardness data are greater than the microhardness values (Fig. 3), in this case increasing by a roughly proportional amount for each mineral. Additionally DSI calculations depend on the contact area of the probe with the sample, so they are more sensitive to imperfections in the probe shape, as well as to harder and stiffer materials than micro-

indentation. Other sources of uncertainty in DSI measurements include determination of the origin of the load-displacement curve (minimum detectable load), the calculation of unloading stiffness (contact stiffness), unknown magnitude of material pile-up around the probe tip, and other aspects of the measuring system and environment (Mencik and Swain 1995).

Toughness values generally increase with Mohs number (see Fig. 3b). The toughness of talc (Mohs number = 1) could not be determined as no radial cracks formed during indentation. Gypsum (Mohs number = 2) exhibited very inconsistent cracking, which, compounded by its propensity for cleaving, prevented an accurate toughness value from being determined. Calcite (Mohs number = 3; $K_{Ic} = 0.39$ MPa m^{1/2}) cracked radially, allowing a toughness value to be determined, as well as in a zigzag manner along cleavage planes (see Fig. 2c). Fluorite (Mohs number = 4; $K_{Ic} = 0.89$ MPa m^{1/2}), apatite (Mohs number = 5; $K_{Ic} = 0.76$ MPa m^{1/2}), and orthoclase (Mohs number = 6; $K_{Ic} = 0.88$ MPa m^{1/2}) all have statistically similar toughness values, about 0.5 MPa m^{1/2} higher than calcite. There is a ~1 MPa m^{1/2} jump to quartz (Mohs number = 7; $K_{Ic} = 1.60$ MPa m^{1/2}) and topaz (Mohs number = 8; $K_{Ic} = 1.04$ MPa m^{1/2}), which also have similar toughness values. The value for corundum (Mohs number = 9, $K_{Ic} = 2.38$ MPa m^{1/2}) is more than twice that of topaz. Novikov and Dub (1991) report the toughness of diamond (Mohs number = 10) as 5 MPa m^{1/2}, twice again the value of corundum.

Modulus values determined by DSI (Table 3) compare closely with literature values determined by a variety of workers and methods (Fig. 3c). Average literature values were calculated using the Voigt and Reuss bounds or the Hashin and Shtrikman bounds, as listed in Simmons and Wang (1971). For calcite through topaz on the Mohs scale, the DSI values are the same or higher than the literature value, but are lower for corundum.

Plots of toughness vs. hardness (Fig. 4a) and modulus vs. hardness (Fig. 4b) highlight how these properties relate to scratch resistance. In the graph of toughness vs. hardness (Fig. 4a), we can see that toughness increases with microhardness (with the exception of topaz) similar to the plot of toughness vs. Mohs number (Fig. 3b). In this graph involving quantitative measurement of hardness, however, it is clear that the Mohs minerals are not evenly spaced in terms of relative hardness. The spacing is relatively tight for calcite, fluorite, apatite, and orthoclase; calcite-fluorite and apatite-orthoclase also have very similar hardness values within each pair. For the remainder of the minerals, the spacing is larger. Additionally, a plot of fracture resistance, R ($R = K_{Ic}^2/E$), vs. Mohs number shows an approximately quadratic trend.

The relationship of modulus to microhardness shows that there is no consistent trend across the Mohs scale (Fig. 4b). Modulus increases dramatically relative to hardness for the first four minerals in the scale (talc, gypsum, calcite, fluorite), but fluorite and apatite have similar values. Orthoclase (feldspar) and quartz, both tectosilicates that represent two of the most important rock-forming minerals in continental crust, have low modulus values that are similar to those of calcite (Fig. 4b, Table 3). Although the microhardness of topaz is only about 5 GPa greater than that of quartz, the modulus of topaz is substantially higher. For hardness, modulus, and toughness, corundum has significantly higher values than any minerals lower on the Mohs scale.

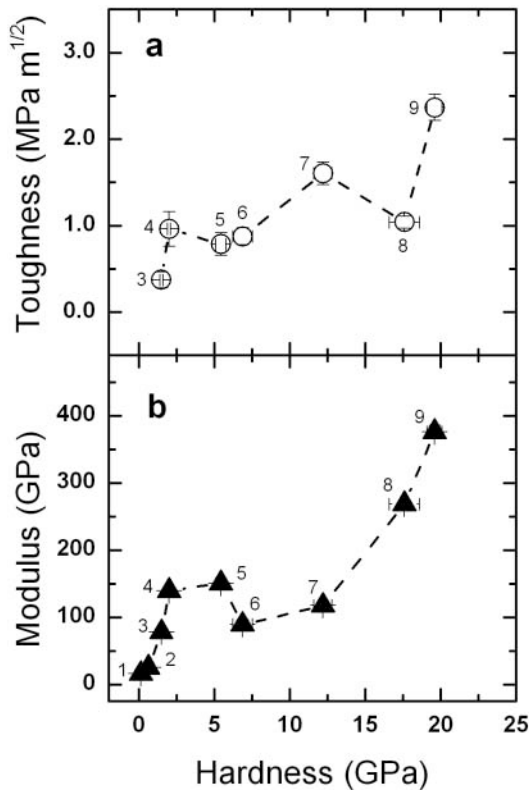


FIGURE 4. (a) Toughness vs. microhardness, (b) experimental modulus vs. microhardness. Mohs numbers are listed next to each data point.

DISCUSSION

Mineral properties and geological applications

Quantitative hardness, toughness, and modulus values for minerals have a wide variety of industrial and biomedical applications, but are also useful for understanding geological processes. Microhardness determined by indentation-based methods can be used to calculate flow laws for minerals, and therefore to study the rheology of these minerals and their host rocks. Indentation hardness has therefore been determined for minerals that are abundant in the crust and mantle; e.g., quartz (Brace 1963, 1964; Darot et al. 1985), olivine (Darot et al. 1985), garnet (Karato et al. 1995), and clinopyroxene (jadeite and diopside: Dorner and Stöckhert 2004). These data are relevant for understanding the brittle behavior of rocks (e.g., earthquake mechanics, Goldsby et al. 2004) and ductile flow of rocks in the crust and mantle (e.g., Karato et al. 1995).

Our measurements were conducted on nominally dry rocks in air at room temperature, but in nature, the hardness of minerals can be affected by environmental factors such as temperature, chemical substitutions (solid solution or impurities), and fluids. The response of mineral hardness to these factors has been well studied for minerals with engineering or medical uses (calcite, apatite, quartz; e.g., Wakeman et al. 1993), and the effect of temperature in particular has been studied for minerals of geological interest (olivine: Evans and Goetze 1979; garnet: Karato et al.

1995; Ca-Na clinopyroxene: Dorner and Stöckhert 2004).

Only three of the Mohs minerals—calcite, orthoclase, and quartz—occur in sufficient abundance to influence the rheology of continental crust. Quartz is the most important, and calcite is locally important where limestone or calcite marble occurs. Orthoclase is significant if its properties are generalized to those of plagioclase feldspar. Talc may also be important locally in subduction zones and in continental regions where talc-bearing serpentinites are present in tectonically active regions. Although the material properties of the remaining minerals may not be relevant to rheological studies, they have other, more specialized applications; e.g., the material properties of apatite, a mineral useful in geochronology and paleontology, may be helpful when interpreting textures and ages of apatite in deformed rocks or in paleontological samples (teeth) that show evidence of wear.

Mineral properties and the Mohs scale

Because of the care that Friedrich Mohs took when selecting common minerals for his scale, each mineral can be distinguished from the others by its relative scratch resistance. Some of the minerals in the scale, however, have very similar microhardness values as determined by indentation experiments (e.g., apatite and orthoclase). This suggests that other properties such as toughness and modulus are also involved in the phenomenon of scratch resistance. Although each of these properties is a complicated function of the crystal chemistry, structure, and bonding characteristics of each mineral, the data suggest that minerals with similar microhardness or toughness can be predicted to have different scratch resistance owing to differences in other properties.

Until the physical processes of cracking associated with scratching vs. indentation are studied in more detail, the best explanation is that scratch resistance is fundamentally different from hardness, and that fracture toughness effects may dominate for some minerals. There is no simple way to predict the relationship of material properties and Mohs number.

The Mohs scale as a teaching tool

Do students need to know the difference between scratch resistance and hardness? Is there a simple way to explain, test, or illustrate what the Mohs scale does measure?

The simplest way to describe accurately the property measured by scratching a mineral is to replace the word “hardness” with “scratch resistance”, refer to the scale as the Mohs scale (not the Mohs hardness scale), and the test as the Mohs scratch test. For more in depth discussions of the physical properties of minerals, however, it is worth understanding the difference between hardness and scratch resistance, and this can be discussed with mineralogy and other students in geoscience classes beyond the introductory level by (1) defining mineral hardness in the context of crystal structure and bonding types, (2) explaining why there is no absolute hardness scale, and (3) showing students the results of indentation experiments and how the results are used to calculate values for material properties. Using Table 3 and the equations described in this paper or other references on hardness and related properties, students can calculate for themselves the hardness and fracture toughness, and plot the results against Mohs number or other variables. The Mohs scale works very

well as a rapid method for determining whether a mineral can be scratched; therefore, it is an excellent way to teach mineral identification techniques.

ACKNOWLEDGMENTS

This research was supported by NSF grant EAR-0106673 to D.L.W. We thank B. Stöckhert, W. Gerberich, and an anonymous reviewer for their helpful comments.

REFERENCES CITED

- Alexandrov, K.S. and Ryzhova, T.V. (1961) The elastic properties of crystals. *Soviet Physics, Crystallography*, 6, 228–252.
- — — (1962) Elastic properties of rock-forming minerals: III feldspars. *Bulletin of the Academy of Sciences of the USSR, Geophysical Series*, 12, 129–131.
- Anstis, G.R., Chantikul, P., Marshall, D.B., and Lawn, B.R. (1981) Evaluation of indentation techniques for measuring fracture toughness: I. Direct crack measurements. *Journal of the American Ceramic Society*, 64, 533–538.
- Brace, W. (1963) Behavior of quartz during indentation. *Journal of Geology*, 71, 581–595.
- — — (1964) Indentation hardness of minerals and rocks. *Neues Jahrbuch für Mineralogie Monatshefte*, 9–11, 257–260.
- Caley, E.R. and Richards, J.E.C. (1956) *On Stones*, 238 p. (translation). Ohio State University Press, Columbus, Ohio.
- Cook, R.F., Lawn, B.R., and Fairbanks, C.J. (1985) Microstructure-strength properties in ceramics, I: Effect of crack size on toughness. *Journal of the American Ceramic Society*, 68, 604–615.
- Darot, M., Gueguen, Y., Benchemam, Z., and Gaboriaud, R. (1985) Ductile-brittle transition investigated by micro-indentation: results for quartz and olivine. *Physics of the Earth and Planetary Interiors*, 40, 180–186.
- Dorner, D. and Stöckhert, B. (2004) Plastic flow strength of jadeite and diopside investigated by microindentation hardness tests. *Tectonophysics*, 379, 227–238.
- Eichholz, D.E. (1971) *Pliny the Elder, Natural History*. Loeb Classical Library (translation), Harvard University Press, Cambridge.
- Evans, B. and Goetze, C. (1979) Temperature variation of hardness of olivine and its implication for polycrystalline yield stress. *Journal of Geophysical Research*, 84, 5505–5524.
- Goldsby, D.L., Rar, A., Pharr, G.M., and Tullis, T.E. (2004) Nanoindentation creep of quartz, with implications for rate- and state-variable friction laws relevant to earthquake mechanics. *Journal of Materials Research*, 19, 357–365.
- Hauy, R.-J. (1822) *Traité de Minéralogie*, ed. 2, vol. 1 pp.136–137. Bachelier, Paris.
- Hearmon, R.F.S. (1946) The elastic constants of anisotropic materials. *Reviews of Modern Physics*, 18, 409–440.
- — — (1956) The elastic constants of anisotropic materials II. *Advances in Physics*, 5, 323–382.
- Hertz, H. (1896) *Miscellaneous Papers* (translated by Jones, D.E. and Schott, G.A.), p. 178–180. Macmillan and Co., Ltd., London.
- Hodge, H.C. and McKay, J.H. (1934) The “microhardness” of minerals comprising the Mohs scale. *American Mineralogist*, 19, 161–168.
- Hooykaas, R. (1970) “Hauy, René-Just,” from *Dictionary of Scientific Biography*, v. VI, p. 178–183. Charles Scribner’s Sons, New York.
- Huntington, H.B. (1958) The elastic constants of crystals. In F. Seitz and D. Turnbull, Eds., *Solid State Physics*, 7, 213–285. Academic Press, New York.
- Karato, S., Wang, Z.C., Liu, B., and Fujino, K. (1995) Plastic deformation of garnets: Systematics and implications for the rheology of the mantle transition zone. *Earth and Planetary Science Letters*, 130, 13–30.
- Khrushchov, M.M. (1949) O vvedanii novoi shkaly tverdsti (On the introduction of a new hardness scale). *Zavodskaja Laboratoriia*, 15, 213–217.
- — — (1950) Microhardness, Mohs hardness and a hardness scale. *Chemical Abstracts*, 44, 10424.
- Knoop, F., Peters, C.G., and Emerson, W.B. (1939) Sensitive pyramidal-diamond tool for indentation measurements. United States National Bureau of Standards, Research Paper RP1220, 39–61.
- Kong, H. and Ashby, M.F. (1992) Wear mechanisms in brittle solids. *Acta Metallurgica et Materialia*, 40, 2907–2920.
- Lawn, B.R., Evans, A.G., and Marshall, D.B. (1980) Elastic/plastic indentation damage in ceramics: the median/radial crack system. *Journal of the American Ceramic Society*, 63, 574–581.
- Mencik, J. and Swain, M.V. (1995) Errors associated with depth-sensing microindentation tests. *Journal of Materials Research*, 10, 1491–1501.
- Mohs, F. (1825) *Treatise on Mineralogy*, 458 p. (translated by W. Haidinger). Caledonian Mercury Press, Edinburgh.
- Novikov, N.V. and Dub, S.N. (1991) Fracture toughness of diamond single crystals. *Journal of Hard Materials*, 2, 3–11.
- Oliver, W.C. and Pharr, G.M. (1992) An improved technique for determining hardness and elastic modulus using load and displacement sensing indentation experiments. *Journal of Materials Research*, 7, 1564–1583.
- Pliny, G. (77) *Historia Mundi*, Book XXXVII.
- Rockwell, S.P. (1922) The testing of metals for hardness. *Transactions of the American Society for Steel Treating*, 2, 1013–1033.
- Simmons, W. and Wang, H. (1971) *Single Crystal Elastic Constants and Calculated Aggregate Properties: A Handbook*, ed. 2, 370 p. The Massachusetts Institute of Technology Press, Cambridge.
- Sisco, A.G. (1956) Réaumer’s *Memoirs on Steel and Iron*, 395 p., 17 plates (translation of original 1722 text). The University of Chicago Press, Chicago.
- Tabor, D. (1951) *The Hardness of Metals*, 175 p. Clarendon Press, Oxford.
- — — (1954) Mohs’s hardness scale—A physical interpretation. *Proceedings of the Physical Society, Section B*, 67, 249–257.
- — — (1970) The hardness of solids. *Review of Physics in Technology*, 1(3), 145–170.
- Taylor, E.W. (1949) Correlation of the Mohs’s scale of hardness with the Vicker’s hardness numbers. *Mineralogical Magazine*, 28, 718–721.
- Wakeman, R.J., Henshall, J.L., and Carter, G.M. (1993) The solution environment effects on the hardness and toughness of calcite during grinding. *Chemical Engineering Research and Design*, 71, 361–370.
- Werner, A.G. (1962) Von den äusserlichen kennzeichen der fossilien (On the external characters of minerals), pp. 93–95, 116–118, translated by A.V. Carazzi. University of Illinois Press, Urbana, Illinois.
- West, G. (1986) An observation on Mohs’ Scale of Hardness. *Quarterly Journal of English Geology*, 19, 203–205.
- Williams, S.R. (1942) Hardness and hardness measurements, 558 p. The American Society for Metals, Cleveland, Ohio.
- Winchell, H. (1945) The Knoop microhardness tester as a mineralogical tool. *American Mineralogist*, 30, 583–595.
- Yoon, H.S. and Newnham, R.E. (1969) Elastic properties of fluorapatite. *American Mineralogist*, 54, 1193–1197.

MANUSCRIPT RECEIVED NOVEMBER 3, 2004

MANUSCRIPT ACCEPTED JUNE 1, 2005

MANUSCRIPT HANDLED BY LEE GROAT